Journal of Electronic Materials (2023) 52:5975–5979
https://doi.org/10.1007/s11664-023-10514-7

ORIGINAL RESEARCH ARTICLE

Effect of Carrier Gas on Silicon Doped GaN Epilayer Characteristics

Jizhong Li[1] · Paul Brabant[1] · Dan Hannan[1] · David Lawson[1]

Received: 27 July 2022 / Accepted: 17 May 2023 / Published online: 17 June 2023

Abstract
Heavily Si-doped GaN epitaxial layers (n^+GaN) have been grown on semi-insulating 6H-SiC substrate by metal–organic chemical vapor deposition at 1030°C using H_2 and N_2 as carrier gases. Thin film characterization results demonstrated that n^+GaN grown in N_2 carrier gas has superior morphological and crystalline quality to that grown in H_2. The surface morphology of n^+GaN grown with N_2 carrier gas is insensitive to the growth rate and SiH_4 flow with Si doping concentration up to $1.1\times10^{20}/cm^3$. Secondary ion mass spectrometry analysis confirmed that C and O impurity levels in n^+GaN are one order of magnitude lower with N_2 carrier gas than with H_2. The results thus indicate that 100% N_2 could be a better carrier gas candidate to enable a broader process window for future HEMT S/D n^+GaN selective area epitaxial process applications.

Keywords GaN · MOCVD · carrier gas · Si doping · morphology

Introduction

Excellent DC and RF device performance have been demonstrated for AlN/GaN high-electron-mobility transistors (HEMTs) on SiC substrates.[1] In order to further reduce the device's total resistance, one technical challenge is the development of high-quality source/drain (S/D) material for ohmic contacts by metal–organic chemical vapor deposition (MOCVD) selective area epitaxy (SAE). To date, H_2 has been the primary choice of carrier gas used in the SAE process of n^+GaN by MOCVD. However, H_2-based SAE overgrowth has a higher growth rate in general and can be 10 times greater than that of unpatterned GaN films due to mass transport and loading effects. As a result, the n^+GaN SAE process usually results in the formation of rough surfaces and even porous films,[2] which promotes the accumulation of dislocations and produces an abrupt, non-uniform doping profile on the sidewalls of S/D regions.[3,4] Therefore, exploring broader MOCVD growth windows for an improved n^+GaN SAE process using an alternative carrier gas, such as mixed H_2 and N_2 or 100% N_2, is highly desirable. However, no research has been reported on the use of 100% N_2 as carrier gas for growing heavily Si-doped GaN materials on SiC substrate.

To better understand the impact of carrier gas dynamics on the n^+GaN SAE process, we first conducted a pilot study by growing n^+GaN on planar substrates. In this presentation, MOCVD growth of n^+GaN on planar SiC substrate was investigated by employing 100% H_2 and 100% N_2 as a carrier gas, individually. The carrier gas's impact on morphology and crystalline quality of n^+GaN has been characterized and compared. It is worth mentioning that the growth conditions reported here had been successfully applied to n^+GaN MOCVD SAE with a proper scaling factor to adjust the growth rate. Detailed electrical characterization results were reported separately.[5]

Experiment

The experimental epitaxy structure was deposited on SI 6H-SiC (0001) substrates by MOCVD using a Thomas Swan CCS reactor with 4×4″ susceptor configuration. Trimethylgallium (TMGa) and trimethylaluminum (TMAl) in combination with ammonia (NH_3) were used as III and V sources, respectively. Silane (SiH_4) diluted to 100 ppm in H_2 was used as the Si dopant source. The base layer structure, depicted in Fig. 1, was grown completely in H_2. Prior to deposition of the base structure, the SiC substrate was baked in H_2 carrier gas at 1080°C and 6.7 kPa torr for

✉ Jizhong Li
Jizhong.li@ngc.com

[1] Advanced Technology Laboratory, Northrop Grumman Corporation, 1212 Winterson Road, Linthicum, MD 21090, USA

10 min to remove the native oxide, followed by the deposition of a 100 nm thick AlN nucleation layer. A 1.5 µm $Al_{0.04}GaN$ buffer layer, a 60 nm GaN layer and finally an 8 nm $Al_{0.25}GaN$ layers were then grown continuously. The 8 nm $Al_{0.25}GaN$ layer served as a marker layer for ensuing characterization involving X-ray reflectivity (XRR) and secondary-ion mass spectrometry (SIMS). Finally, the base layer structure was capped by an n^+GaN layer with a target thickness of 20 nm, whose process conditions are summarized in Table I.

The experiments consist of two groups of n^+GaN samples. Samples whose n^+GaN caps were grown in H_2 are categorized as Group-1, and those grown in N_2 are Group-2. The target thickness of 20 nm n^+GaN was achieved by adjusting growth time and $TMGa/NH_3$ flows while maintaining a constant V/III ratio. SiH_4 flow was proportionally scaled to match each growth rate. In Group-2, the main carrier gas was switched and ramped from H_2 to N_2 prior to growth of n^+GaN while the total gas flow to the process chamber remained the same to maintain stable chamber pressure. In this study, the amount of H_2 passing through TMGa, TMAl bubblers and SiH_4 source lines are small vs. total gas in growth chamber ($H_2/N_2 < 0.5\%$) and its effect on main N_2 carrier gas is minimal. The n^+GaN layer thickness and growth rate were obtained by XRR. Surface morphology of n^+GaN was investigated by atomic force microscopy (AFM). Si doping and background impurity concentrations were analyzed by SIMS.

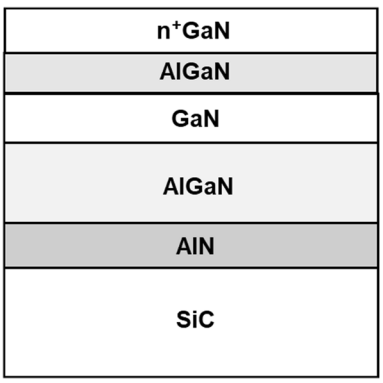

Fig. 1 Schematic structure of blanket base layer grown on bare SiC substrate using H_2 as carrier gas.

Results and Discussion

Figure 2 shows the XRR data analysis for n^+GaN thickness characterization. Experimental curves were simulated using commercial BEDE RADS software. Oscillations on the reflectivity curves, which are due to the $n^+GaN/AlGaN$ interfaces, are clearly visible. For the samples referenced in Fig. 2 column (a), sample #1H was grown without Si doping, used as a reference for surface morphology evaluation for Group-1. Sample #2H is Si doped with SiH_4 flow of 225 sccm, corresponding to a Si doping concentration of $9.9\times10^{19}/cm^3$. To verify growth rate linearity, the growth rate of sample #1H was set to one-third of that of sample #2H for the same layer thickness. Samples in Fig. 2 column (b) were selected from Group-2. For direct comparison, samples #1N and #2N used the same process settings as used for #1H and #2H, respectively, except for the carrier gas.

To confirm the impact of the carrier gas on n^+GaN growth rate, SIMS analysis was conducted on samples #2H and #2N. As seen in Table I, the thickness values agreed reasonably well. This was determined by comparison to the XRR fitting results of both samples. The n^+GaN growth rate

Table I n^+GaN growth parameters and characterization results

Carrier gas	Sample#	Growth T (°C)	SiH_4 (sccm)	Growth rate (Å/s)	AFM 10×10 RMS (Å)	XRR thickness (Å)	SIMS thickness (Å)	[Si] (cm^{-3})	[O]	[C] (cm^{-3})
H_2 (Group-1)	1H	1030	0	1.7	6.12	218	*	*	*	*
	2H	1030	225	5.1	8.15	216	220	9.9×10^{19}	5.3×10^{18}	7.7×10^{18}
	3H	1030	50	1.7	16.8	–	*	*	*	*
	4H	1030	75	1.7	25.4	–	*	*	*	*
						–				
	5H	950	150	5.1	17.8	–	*	*	*	*
	6H	950	225	5.1	57.9	–	*	7.3×10^{19}	3.2×10^{19}	3.5×10^{19}
N_2 (Group-2)	1N	1030	0	1.5	6.99	176	*	*	*	*
	2N	1030	225	4.5	4.18	178	180	1.1×10^{20}	7.5×10^{17}	6.6×10^{17}
	3N	1030	85	1.5	4.63	–	*	*	*	*
	4N	1030	95	1.5	4.64	–	*	*	*	*

*Not determined

Si, O, C data were taken at depth 14 nm to avoid surface contamination diffusion

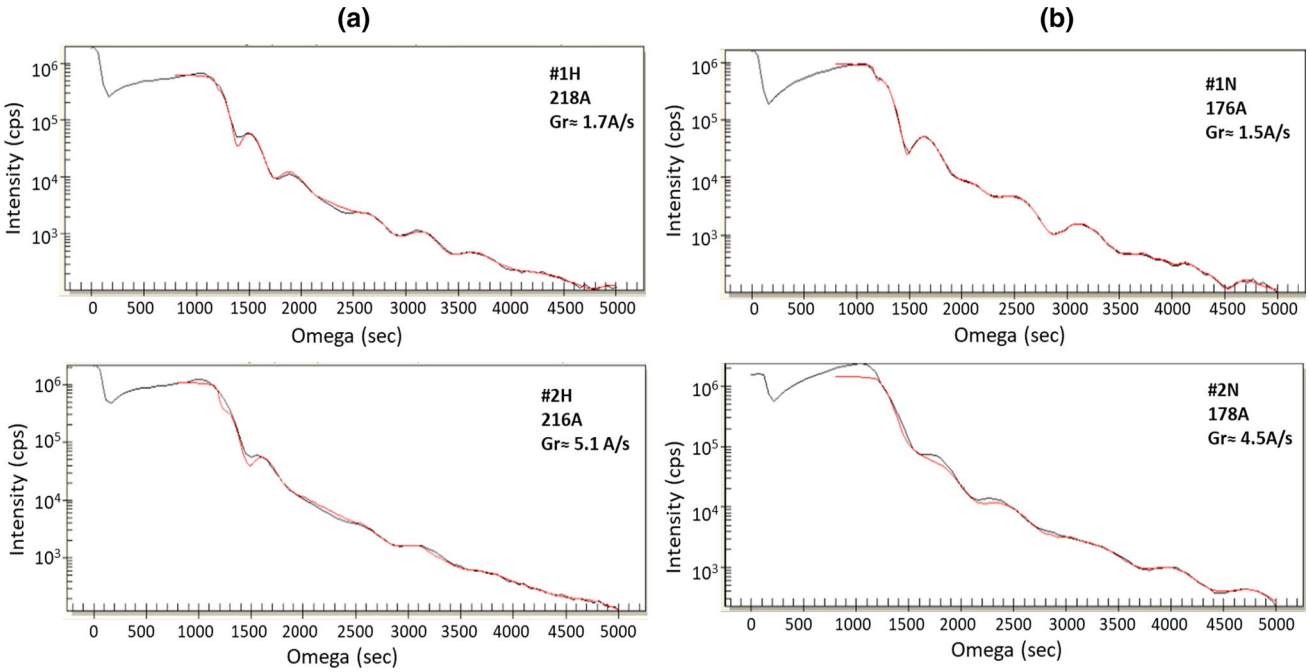

Fig. 2 Experimental and simulated X-ray reflectivity curves of n^+GaN/AlGaN structures. Black lines are experimental data and red lines are simulation curves. Samples in column (a) were grown using H_2 as carrier gas and in column (b) using N_2 as carrier gas.

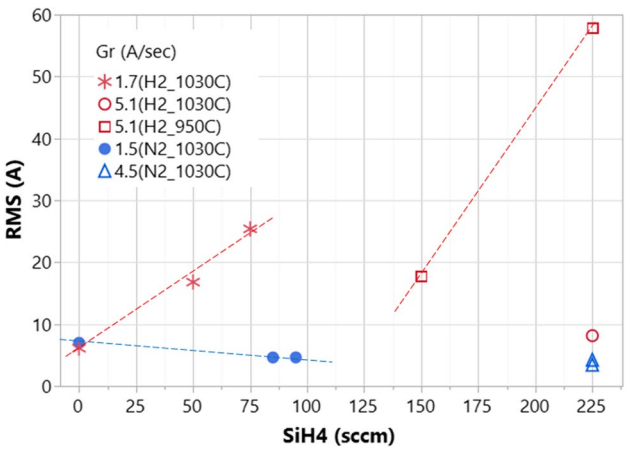

Fig. 3 Dependence of n^+GaN surface AFM RMS on SiH_4 flow, growth rate, growth temperature and carrier gasses.

in N_2 carrier gas is about 20% lower than that in H_2 carrier gas. These results are comparable to the general trend as reported,[6–8] with discrepancies attributed to the differences in MOCVD reactor configuration and growth conditions.

Figure 3 reports the AFM root mean square (RMS) values with respect to the experimental designs listed in Table I. Data plotted in red indicate samples from Group-1, while data in blue represent Group-2. With H_2 carrier gas, Si-doped n^+GaN roughness RMS values are strongly dependent on growth temperature, SiH_4 flow, and growth rate. In particular, for the same growth rate and SiH_4 flow, reducing the growth temperature from 1030°C to 950°C caused an increase in RMS by nearly one order of magnitude and a 26% decrease in Si concentration.

In the experiments, Si incorporation was intentionally increased towards its saturation level.[9] The strong temperature effect on the surface morphology could be explained by a thermodynamic model.[10] For SiH_4-doped GaN grown by MOCVD, the critical temperature is about 950°C. Incomplete pyrolysis of SiH_4 in mixed H_2 carrier gas occurs below this temperature, where limited Si incorporation efficiency and surface roughening effects are observed, even at a lower SiH_4 flow. This phenomenon is represented by the two square-shaped data points shown in Fig. 3.

It has been reported that for undoped GaN growth, the carrier gas impacts surface stoichiometry significantly, and H_2 is more temperature-sensitive to the surface growth mode.[11] The stoichiometry is more complicated during n^+GaN growth, as the Si dopant introduces additional tensile stress and higher dislocation density with alternate surface reconstruction dynamics.[12] As a result, n^+GaN surface morphology and layer quality are determined by the stage of mode transition which relies on factors including growth temperature, Si doping level, growth rate and layer thickness. This could explain the challenge in improving n^+GaN surface morphology with H_2 carrier gas.

However, for samples in Group-2, data show that the effect of the growth rate and SiH_4 flow on surface roughness

is negligible. Blue dots in Fig. 3 show that the RMS value decreases with increasing SiH_4 flow up to a Si concentration of $1.1\times10^{20}/cm^3$. The maximum RMS of 6.99 Å was measured from sample #1N without doping. This may explain why 100% N_2 has been reported to be detrimental to the morphology, from which only undoped GaN growth has been investigated.[13,14]

Figure 4 shows 10 µm × 10 µm AFM roughness images taken from the center of the wafers grown at 1030°C. As seen in Fig. 4a, Si-induced defect clusters were observed across the wafer surface grown with H_2 carrier gas, contributing to large RMS illustrated by the red plots in Fig. 3. When using N_2 carrier gas, cluster defect features were no longer observed, and small dark pits were observed across the smooth surface with uniform size distribution. As seen from left to right in Fig. 4b, pit density increased with increasing SiH_4 flow, but pit size remained unchanged. Additional experiments not reported here indicate that thicker n^+GaN grown in N_2 resulted in a pit-free surface, suggesting that the 20 nm n^+GaN layer used in this study was not fully coalesced.

Figure 5 depicts SIMS results of samples #2H and #2N at a sputtering depth slightly below the 8 nm AlGaN marker layer. As shown in Table I, both samples achieved a Si concentration level of around $1\times10^{20}/cm^3$, which means that Si incorporation efficiencies are essentially the same for n^+GaN growth with either carrier gas. However, impurity concentrations of C and O within the doped GaN capping layer are significantly different. For sample #2N, the concentration levels of C and O are $6.6\times10^{17}/cm^3$ and $7.5\times10^{17}/cm^3$, respectively. For sample #2H, the corresponding levels are an order of magnitude higher, at $7.7\times10^{18}/cm^3$ and

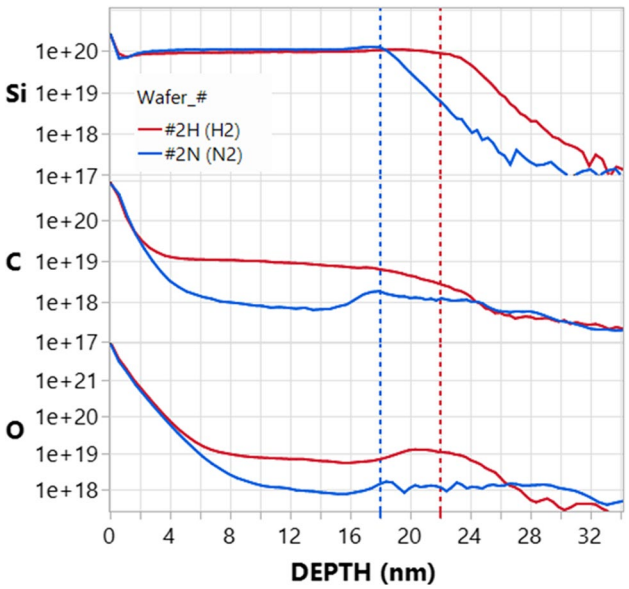

Fig. 5 SIMS results comparison for Si, C and O impurity concentrations as a function of sputter depth in n^+GaN/AlGaN structures. Sample #2H was grown in H_2 carrier gas and sample #2N was grown in N_2 carrier gas.

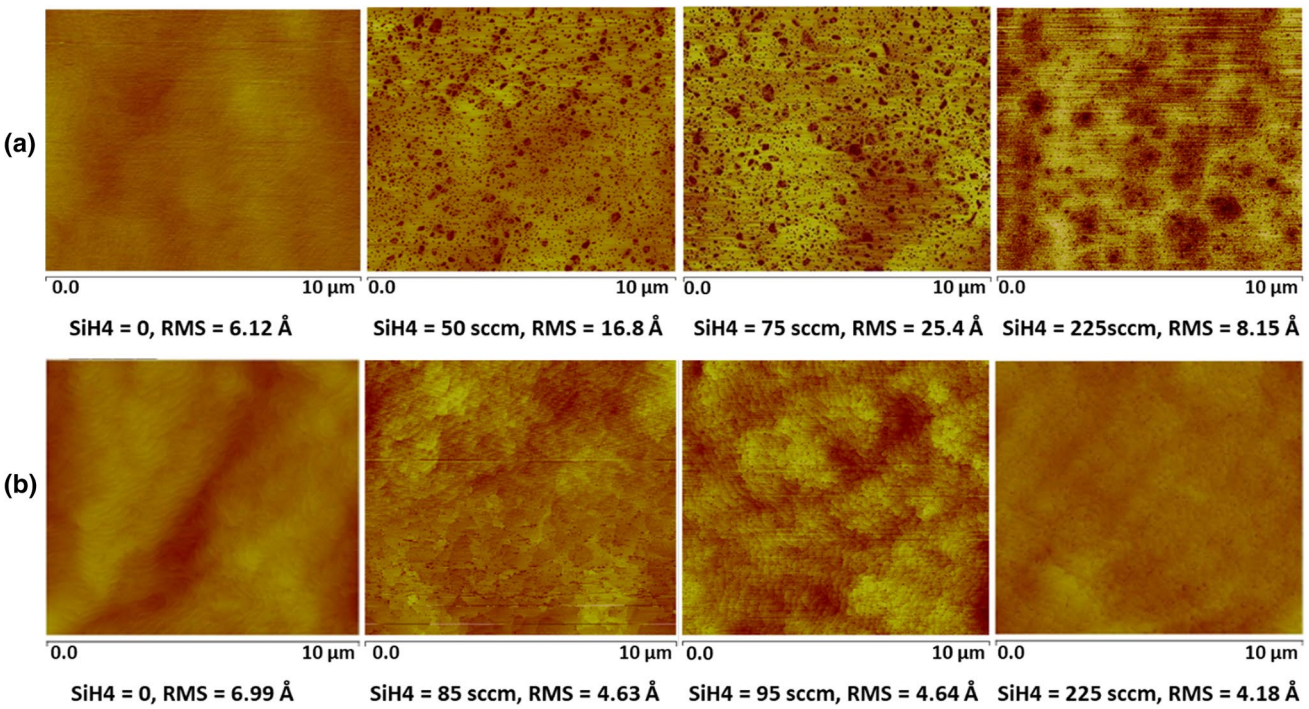

Fig. 4 10 µm × 10 µm AFM images of n^+GaN grown on SiC substrate using (a) H_2 as carrier gas and (b) N_2 as carrier gas.

$5.3 \times 10^{18}/cm^3$, respectively. We attribute this improvement to the following: (1) n^+GaN grown in N_2 carrier gas results in an effectively higher V/III ratio due to higher cracking of NH_3, which helps suppress O incorporation, and[6] (2) n^+GaN grown in N_2 carrier gas has a N-rich surface. This surface structure greatly reduces the possibility of N vacancy formation. As a result, the chances of N vacancy occupation by CH_3 radicals, which is the impurity source of C, are reduced.[15]

Supported by the data presented in Figs. 3, 4, and 5, the improvement in n^+GaN surface morphology when using N_2 carrier gas is attributed to surface stoichiometry difference stemming from the lack of deleterious effects. However, the mechanisms underlying the impact of Si on n^+GaN morphology and material quality when using 100% N_2 carrier gas are still not fully understood, and further investigations are currently underway.

This work demonstrated n^+GaN MOCVD growth on 6-H SiC substrate with superior surface morphology using N_2 as carrier gas. We observed that Si doping improved GaN surface morphology vs. undoped GaN with N_2 carrier gas, up to an incorporation density of $1.1 \times 10^{20}/cm^3$. The improvement in morphology is believed to be the result of the change in surface stoichiometry related due to SiH_4 implementation. The surface roughness seems to be improved with a higher incorporated amount of Si. In contrast, the same growth conditions in H_2 carrier gas proved deleterious to n^+GaN morphology. Data also showed that n^+GaN growth in N_2 carrier gas resulted in C and O impurity concentrations one order of magnitude lower than that with H_2 carrier gas. These results suggest that using 100% N_2 as carrier gas would be a promising approach for future HEMT S/D n^+GaN SAE growth.

Conflict of interest The authors declare that they have no conflict of interest.

References

1. R.S. Howell, E.J. Stewart, R. Freitag, J. Parke, B. Nechay, H. Cramer, M. King, S. Gupta, J. Hartman, M. Snook, I. Wathuthanthri, P. Ralston, K. Renaldo, H.G. Henry, and R.C. Clarke, The Super-Lattice Castellated Field Effect Transistor (SLCFET): A novel high performance Transistor topology ideal for RF switching, in *IEEE Electron Devices Meeting* (IEDM), 2014. https://doi.org/10.1109/IEDM.2014.704703
2. Y.N. Saripalli, C. Zeng, J.P. Long, D.W. Barlage, M.A.L. Johnson, and D. Braddock, Properties of III-N MOS Structures with Low-temperature Epitaxially Regrown Ohmic Contacts. *J. Cryst. Growth* 287, 562 (2006).
3. C.C. Mitchell, M.E. Coltrin, and J. Han, Mass Transport in the Epitaxial Lateral Overgrowth of Gallium Nitride. *J. Cryst. Growth* 222, 144 (2001).
4. H. Fu, K. Fu, C. Yang, H. Liu, K.A. Hatch, P. Peri, D.H. Mudiyanselage, B. Li, T.-H. Kim, S.R. Alugubelli, P.-Y. Su, D.C. Messina, X. Deng, C.-Y. Cheng, R.V. Meidanshahi, X. Huang, H. Chen, T.-H. Yang, and Y. Zhao, Selective Area Regrowth and Doping for Vertical Gallium Nitride Power Devices: Materials Challenges and Recent Progress. *Mater. Today* 49, 296 (2021).
5. J. Li, P. Brabant, D. Hannan, T. Vasen, S. Afroz, K. Nagamatsu, J. Chang, P. Shea, D. Lawson, and R.S. Howell, Ultra-low Resistance n+GaN Contacts for GaN HEMT Applications Using MOCVD Selective Area Epitaxy in N2 Carrier Gas. *AIP Adv.* 12, 035201 (2022).
6. X. Su, T. Ye, S. Wang, Y. Shi, L. Fan, L. Liu, G. Zhang, X. Shi, M. Wei, H. Zhou, and H. Jiao, Surface Morphology of GaN Nucleation Layer Grown by MOCVD with Different Carrier Gas. *AIP Adv.* 8, 075301 (2018).
7. Y.S. Cho, H. Hardtdegen, N. Kaluza, N. Thillosen, R. Steins, Z. Sofer, and H. Lüth, Effect of Carrier Gas on GaN Epilayer Characteristics. *Phys. Stat. Sol. C* 3(6), 1408 (2006).
8. O. Jumaah and Y. Jaluria, The Effect of Carrier Gas and Reactor Pressure on Gallium Nitride Growth in MOCVD Manufacturing Process. *J. Heat Transf.* 141, 082101 (2019).
9. I. Halidou, Z. Benzarti, Z. Chine, T. Boufaden, and B. El Jani, Heavily Silicon-doped GaN by MOVPE. *Microelectron. J.* 32, 137 (2001).
10. A. Toure, I. Halidou, Z. Benzarti, and T. Boufaden, Growth Temperature Effect on MOVPE Si-doped GaN: Thermodynamic Modeling. *Microelectron. J.* 40, 363 (2009).
11. Y. Kobayashi and N. Kobayashi, Influence of N_2 Carrier Gas on Surface Stoichiometry in GaN MOVPE Studied by Surface Photoabsorption. *J. Cryst. Growth* 189, 301 (1998).
12. M.A. Moram, M.J. Kappers, F. Massabuau, R.A. Oliver, and C.J. Humphreys, The Effects of Si Doping on Dislocation Movement and Tensile Stress in GaN Films. *J. Appl. Phys.* 109, 073509 (2011).
13. O. Schon, B. Schineller, M. Heuken, and R. Beccard, Comparison of Hydrogen and Nitrogen as Carrier Gas for MOVPE Growth of GaN. *J. Cryst. Growth* 189, 335 (1998).
14. H.X. Wang, Y. Amijima, Y. Ishihama, and S. Sakai, Influence of Carrier Gas on the Morphology and Structure of GaN Layers Grown on Sapphire Substrate by Six-wafer Metal Organic Chemical Vapor Deposition System. *J. Cryst. Growth* 233, 681 (2001).
15. J.L. Zhang, J.L. Liu, Y. Pu, W.Q. Fang, M. Zhang, and F. Yi, Jiang, Effects of Carrier Gas on Carbon Incorporation in GaN. *chin. Phys. Lett.* 31(3), 037102 (2014).